HHS Public Access

Author manuscript

Pediatr Blood Cancer. Author manuscript; available in PMC 2015 December 16.

Published in final edited form as:

Pediatr Blood Cancer. 2012 December 15; 59(7): 1173–1179. doi:10.1002/pbc.24232.

Pediatric brainstem gangliogliomas show overexpression of neuropeptide prepronociceptin (PNOC) by microarray and immunohistochemistry

Mike H. Chan, B.A.[1], **B. K. Kleinschmidt-DeMasters, M.D.**[2,3,4], **Andrew M. Donson, B.S.**[1], **Diane K. Birks, M.S.**[4], **Nicholas K. Foreman, M.D.**[1], and **Sarah Z. Rush, M.D.**[1]

[1]Department of Neuro-oncology, Children's Hospital Colorado, Aurora, Colorado, 13123 East 16th Avenue, Aurora, CO 80045

[2]Department of Pathology, Anschutz Medical Campus, University of Colorado at Denver, 12800 East 19th Avenue, Aurora, CO 80045, USA

[3]Department of Neurology, Anschutz Medical Campus, University of Colorado at Denver, 12800 East 19th Avenue, Aurora, CO 80045, USA

[4]Department of Neurosurgery, Anschutz Medical Campus, University of Colorado at Denver, 12800 East 19th Avenue, Aurora, CO 80045, USA

Abstract

Background—Gangliogliomas (GGs) primary to brainstem are rare, with the overwhelming majority of GGs occurring in supratentorial, especially temporal lobe, locations. A less favorable prognosis exists for brainstem GGs, despite their usually-identical WHO grade I status. Few large clinical series, and limited biological information, exists on these tumors, especially gene expression.

Procedure—Seven pediatric brainstem GGs, all with classic histological features, seen at our institution since 2000 were identified. Frozen section material was available for gene expression microarray profiling from 5 of 7 brainstem GGs and compared with that from 3 non-brainstem pediatric GGs.

Results—Significant upregulation of a number of genes was identified, most of which were involved in pathways of embryogenesis, organogenesis, axis formation, and patterning. The single largest upregulated gene was a 256-fold increase in the expression of the neuropeptide prepronociceptin (PNOC); the protein product of this gene has been implicated in neuronal growth. Overexpression was validated by Western blot and by immunohistochemistry (IHC). Strong IHC expression of PNOC was seen in neoplastic neurons of 7/7 brainstem GGs, but was significantly weaker in non-brainstem GGs, and completely negative in normal pediatric autopsy brainstem controls.

Conclusions—PNOC IHC was often superior to IHC for NeuN, synaptophysin, or neurofilament for highlighting neoplastic neurons.

Corresponding author: Sarah Rush, M.D., Children's Hospital Colorado, 13123 E. 16th Avenue, Aurora, CO 80045, Phone: 720-777-8314, Fax: 720-777-7226, Sarah.Rush@childrenscolorado.org.

Keywords

Ganglioglioma; microarray; immunohistochemistry; neuropeptide; prepronociceptin

INTRODUCTION

Gangliogliomas (GGs) are relatively uncommon mixed glial-neuronal neoplasms that account for approximately 0.5–2% of all central nervous system (CNS) tumors and 1–4% of pediatric CNS tumors [1]. Diagnosis occurs at a mean age of 22 years, with a slight male predominance [2]. GGs are virtually all low grade, World Health Organization (WHO) grade I neoplasms and only rarely exhibit high grade features (i.e., anaplastic GG, WHO grade III) [3]. Criteria for WHO grade II tumors have yet to be established and are not included in the 2007 WHO classification scheme [3].

As expected for a WHO grade I neoplasm, GGs are generally cited as having a relatively favorable prognosis [4], and usually treated by surgical excision alone, without adjuvant therapy. However, the overall favorable prognosis may be significantly influenced by the strong predilection for most GGs to occur in the temporal lobe (86%) [3], an anatomical site that lends itself to total or near-gross total surgical tumor resection. Other supratentorial regions are far less often affected, with involvement of the frontal lobe in only 7% of cases, parietal and occipital lobes in 3% of cases each, multiple lobes in 7%, and ‘other’ sites constituting 1% [3]. Brainstem GGs are included in these rare ‘other’ GGs, and thus, relatively few studies have been published on this entity [5–9].

Despite the paucity of reports on brainstem GGs, they appear to exhibit significantly different behavior from their supratentorial counterparts. A 1993 study by Lang and colleagues examining the clinical progression of 58 GG patients, reported that patients with GGs in brainstem had a shorter mean duration of symptoms (1.25 years) when compared to cerebral and spinal cord GGs (6 and 1.4 years, respectively) [10]. Following surgical resection of the tumor, only 78% of brainstem GG patients were alive at the time of follow-up evaluation, compared to 89% and 87% for cerebral and spinal cord GG patients, respectively. Patients with brainstem GGs were also shown to have a significantly elevated risk of tumor recurrence or death, when compared to patients with both cerebral and spinal cord tumors [10].

It is unclear if the difference in outcome in brainstem GGs relates solely to the inability to achieve favorable anatomical resection or is due to true biological differences between brainstem and non-brainstem counterparts. Since the current outcome for brainstem GGs is less favorable than that for non-brainstem GGs, often chemotherapy and radiotherapy are necessary as adjuvant therapies. However, even with these standard adjuvant therapies, prognosis remains poorer than for supratentorial counterparts, suggesting that new therapeutic regimens may be required to improve prognosis. Targeted therapies would be particularly attractive, should potential candidates be identified.

We utilized gene expression microarray analyses to search for relevant overexpressed genes in this rare subset of GGs. After gene identification, the highest over-expressed gene, PNOC

(prepronociceptin) was confirmed for protein expression by Western blot and by immunohistochemistry analyses. We directly compared the utility of PNOC IHC with standard synaptophysin, NeuN, and anti-neurofilament IHC in diagnosing neoplastic neurons in brainstem GGs.

METHODS

Patient samples for brainstem GGs, non-brainstem GGs, and controls

Brainstem GG samples were obtained from seven children who presented to Children's Hospital Colorado (Aurora, CO) between 2000 and 2009 incompliance with Colorado Multiple Institutional Review Board (COMIRB) regulations (Table I). Three of the patients were male and four were female ranging in age from 3–13 years (median 4 years). Most common presenting symptoms included features of brainstem involvement such as respiratory distress, soft voice, and weakness. After diagnosis of GG of the brainstem, patients were treated with radiation alone (1 case), or both chemotherapy and radiation (6 cases) (see Table I). Three of the patients progressed following treatment, with a median time to progression of 11.5 months. All cases were classified as WHO grade I and manifested classic histological features of GG on light microscopy, with numerous cytologically-atypical neurons, low grade glial component, perivascular non-neoplastic lymphocytic cuffing, and variable numbers of eosinophilic granular bodies and Rosenthal fibers [3] (Fig. 1a). Although distinguishing true GGs from diffuse infiltrating astrocytomas of brainstem with entrapped non-neoplastic neurons can be diagnostically challenging on small biopsies in some cases, all 7 cases had had significant amounts of tissue resected for confident histological diagnosis. All manifested large numbers of neoplastic ganglion cells and the additional accompanying histological and immunohistochemical features seen in GGs and not diffuse astrocytomas.

For light microscopy, formalin-fixed, paraffin embedded tumor sections were cut at 5 microns and stained with hematoxylin and eosin (H&E) and further immunostained for routine diagnostic immunohistochemical markers including MIB-1 (Dako Corporation, Carpinteria, CA, USA, monoclonal, 1:400 dilution, antigen retrieval), glial fibrillary acidic protein (GFAP; Dako Corporation, polyclonal, 1:2500, no antigen retrieval), synaptophysin (Biogenex, Fremont, CA, monoclonal, 1:50, no retrieval), anti-neurofilament (Cell Marque, Rocklin, CA, monoclonal, pre-diluted, antigen retrieval), and NeuN (Chemicon, Billerica, MA, monoclonal, 1:100, antigen retrieval).

The comparison cohort for PNOC immunohistochemistry studies consisted of 5 pediatric non-brainstem GGs from our institution (Supplemental Table I) and control brainstem sections from 5 pediatric autopsies in which the patients had succumbed to non-neurological causes. Ages and gender for the non-brainstem GGs utilized as the comparison cohort overlapped with those of the brainstem GG cohort and included a 2-year-old male with a left hypothalamic/thalamic GG, a 5-year-old female with a cerebellar GG, a 6-year-old female with a right frontal GG, a 13-year-old male with a left temporal lobe GG, and a 17-year-old male with a suprasellar/hypothalamic GG (Supplemental Table I).

Non-GG controls consisted of normal autopsy brainstem sections from all three levels of brainstem (midbrain, pons, and medulla). Ages and gender for the controls overlapped with the GG cohorts and included a 7-month old male, 7-month-old female, 3 year-old female, 13 year-old male, and 14 year old female. No control patient succumbed to a primary or metastatic brain tumor or a neurological disorder.

Gene expression microarray analysis of tumor specimens

Five micrograms of RNA extracted from tumor was amplified, biotin-labeled (Enzo Biochem), and hybridized to Affymetrix HGU133 Plus 2 microarray chips. Analysis of gene expression microarray data was performed using Bioconductor functions written in the R programming language (www.bioconductor.org). Microarray data were background corrected and normalized using the guanine cytosine robust multiarray average (gcRMA) algorithm, resulting in $\log_2$ expression values. The Affymetrix HGU133 Plus 2 microarray contains 54,675 probe sets, including multiple probe sets for the same gene.

Ontology analysis of microarray data

DAVID (Database for Annotation, Visualization, and Integrated Discovery, http://david.abcc.ncifcrf.gov) ontology analysis was used in this study to assess gene lists for enrichment of genes annotated with specific Gene Ontology Project terms (GOTERM; www.geneontology.org). Briefly, DAVID is a web-based resource that provides Gene Ontology term enrichment scores for lists of genes that have already been identified by the user as significantly associated with a particular phenotype or variable [11]. Enrichment is defined as more genes than would be expected by chance that are associated with a specific phenotype or variable [11,12].

Western blot analysis

Tumor protein lysates were obtained from snap-frozen tumor specimens of 5 pediatric brainstem GGs and 4 pediatric supratentorial GGs. Approximately 30 mg of frozen tumor specimen was homogenized using a PowerGen 125 homogenizer (Fischer Scientific, Waltham, MA) on ice in 1 mL RIPA buffer (Fischer Scientific, Waltham, MA: 25 mM Tris-HCl [pH 7.6], 150 mM NaCl, 1% NP-40, 1% sodium deoxycholate, 0.1% SDS), 1 mM sodium vanadate, and 1 mM sodium molybdate with a complete Mini Protease Inhibitor Cocktail [Roche, Indianapolis, IN].

Forty micrograms of the resulting protein lysates were then incubated with a loading dye, separated on precast 4–20% Criterion sodium dodecyl sulfate Tris-glycine gel (BioRad, San Diego, CA) and transferred to a polyvinylidene difluoride membrane (Millipore, Billerica, MA). Membranes were incubated with rabbit polyclonal anti-PNOC antibody (Proteintech, Chicago, IL) in 3% bovine serum albumin blocking agent or goat polyclonal anti-alpha-tubulin antibody (Cell Signaling Technology, Danvers, MA) in 5% milk at dilutions of 1:250 and 1:1000, respectively, for one hour at room temperature. After incubation with secondary horseradish peroxidase-conjugated donkey anti-rabbit antibody (1:4000 dilution) (Jackson ImmunoResearch Laboratories, West Grove, PA), immunoreactive signals of the protein bands were detected using enhanced chemiluminescence (PerkinElmer, Boston, MA)

detection solution and exposed to X-Omat Blue XB-1imaging film (Eastman Kodak, Rochester, NY).

Immunohistochemistry (IHC) for PNOC

Immunohistochemistry was performed on 5μm formalin-fixed, paraffin-embedded tumor tissue sections using the Leica Bond Refine Detection kit. All steps were done on the BOND machine. Briefly, sections were incubated in citrate buffer high pH 9 (Leica) for 20 minutes at 90 degrees, and then blocked with FC Block (Innovex) and Protein Block (Open Biosystems) for 20 minutes and 5 minutes, respectively. Sections were then stained with primary anti-human orphanin/PNOC antibody (Neuromics #RA10106) at a 1:1000 dilution for 1 hour, followed by treatment with labeled polymer (Leica) for 10 minutes, hydrogen peroxide (Leica) for 10 minutes, and DAB (Leica) for 10 minutes. Sections were then counterstained with hematoxylin (Leica) for 1 minute.

Immunohistochemistry for PNOC was performed on the same tissue block as that utilized for diagnostic immunostaining for synaptophysin, NeuN, and neurofilament so that direct comparison of the quality of staining in similar or identical sections of tumor could be made on serially-cut sections. Scoring was subjective on a subjective scale with +++ = strong and diffuse in large numbers of neurons, ++ = strong in a subset of neurons, + = weak and diffuse, +/− = rare neurons with weak immunoreactivity, and 0 = none.

RESULTS

Clinicopathological features

Clinical presentations for brainstem GG are listed in Table I. All required radiotherapy, or were treated with radiotherapy and chemotherapy. Six of 7 experienced recurrences and 2 of 7 are deceased. All contained significant numbers of neoplastic neurons (Fig. 1a). Tumors showed varying amounts of non-neoplastic perivascular lymphocytes (Fig. 1a), eosinophilic granular bodies, and Rosenthal fibers. Neoplastic neurons manifested variable IHC positivity for synaptophysin and to a lesser extent for NeuN. Neurofilament was generally identified in the abundant axonal processes in the lesions and far less often in the perikaryon of the neoplastic neurons. The only notable histological feature was that most brainstem GGs failed to exhibit large amounts of calcifications. Tumors were histologically otherwise very similar to the comparison non-brainstem GG cohort.

Gene expression analysis

Multiple genes were found to be significantly overexpressed by gene expression microarray profiles in brainstem GGs. A list of the ten most highly overexpressed and underexpressed genes in brainstem GGs is included in Table II.

Differential gene expression data from brainstem GGs was subjected to analysis using DAVID Ontology. The top 50 overexpressed genes, according to fold change, in brainstem GGs were analyzed to detect any possible relevance to tumor biology. This analysis revealed that these genes were involved in pathways of embryogenesis, organogenesis, axis formation, and patterning (Table III). In order to determine if this developmentally-primitive

expression pattern was indeed a function of developmental dysregulation within the tumor itself, and not a byproduct of normal differentially-expressed developmental determinants, we compared microarray data from normal frontal lobe samples (n=3) and normal brainstem samples (n=3) (data not shown). Using this comparison, we were able to determine a baseline of differential gene expression which confirmed that the list of over- and under-expressed genes in the GGs was characteristic of the tumor, and not the normal tissue from the anatomical site of origin.

The single-most differentially-expressed gene in the brainstem GGs was the transcript for the neuropeptide precursor protein, prepronociceptin (PNOC), which was expressed at a 284-fold higher level than in supratentorial counterparts (Table II). Previous studies have shown PNOC to be involved in the process of neurite outgrowth [13–16]. In order to see whether the relatively high PNOC expression in brainstem GGs could be associated with neurite outgrowth, we compared the microarray data for 17 neuronal growth-associated proteins (nGAPs) identified by Lu et al. [17]. These 17 proteins have been shown to be involved in neurite outgrowth in multiple neuronal cell types *in vitro*, and are hypothesized to be markers for the neuron growth cone. Using the same microarray data analysis protocol as described previously, our comparison showed nGAP genes to be modestly upregulated in brainstem GGs in almost all cases, though only 6 of the 17 genes in question were upregulated by a statistically significant margin (Supplemental Table II).

Immunohistochemistry for PNOC

Immunohistochemical staining for PNOC protein revealed strong (+++) expression in large numbers of neoplastic neurons in all 7 of the brainstem GGs (Fig. 1b). Immunostaining was predominantly cytoplasmic and was distributed throughout the cytoplasm rather than in a membranous pattern (Fig. 1b, 1c). In general, the majority of the neoplastic neurons showed immunoreactivity (+++ in scoring scheme). Weak to moderate nuclear immunoreactivity was also noted in nuclei of neoplastic neurons, and occasional glial cells as well.

Careful matching of serial sections taken from the same tissue block from the same case was undertaken to directly compare similar areas of the tumor in terms of quality of PNOC (Fig. 1c), versus NeuN (Fig. 1d), synaptophysin (Fig. 1e), and neurofilament (Fig. 1f) IHC for identifying neoplastic neurons. PNOC (Fig. 1c) highlighted the cell body, similar to NeuN (Fig. 1d) but showed immunostaining in a considerably larger number of the neoplastic neurons. PNOC immunoreactivity was also seen in at least as many, and in some cases, more neoplastic neurons than with synaptophysin IHC (Fig. 1e).

PNOC immunoreactivity was diffusely distributed throughout the cytoplasm in brainstem GGs (Figs 1b, c) rather than simply at the cell membrane, as can be the case with synaptophysin (Fig. 1e), especially when located within strongly synaptophysin-positive gray matter regions (Fig. 1e). Because of the larger volume of cytoplasmic immunoreactivity, PNOC also appeared to be superior in identifying smaller-sized neoplastic neurons as compared to synaptophysin, although roughly equivalent for very large dysplastic neurons. PNOC was far superior in terms of identifying numbers of neoplastic neurons as compared with immunostaining for neurofilament which predominantly highlighted axons and not cell bodies (Fig. 1f). Indeed, unlike neurofilament

immunohistochemistry that decorates axons and only occasional cell perikarya in GGs, PNOC did not appear to decorate axonal processes at all.

In comparison, PNOC IHC in non-brainstem GGs was similar to that in brainstem GGs in only 1 of 5 cases (Fig. 1g), although even in this example the number of immunoreactive neurons appeared fewer than with brainstem GGs (scored as ++). PNOC IHC was significantly weaker and more infrequent in the remaining 2 of 5 non-brainstem GGs (Fig. 1h, scored as +) and only rare (scored as +/−) in the other 2 cases (see Supplemental Table I).

No observable PNOC expression was found in any brainstem neurons at any level (midbrain, pons, medulla) of control autopsy specimens (Fig. 1i, basis pontis control section illustrated, scored as 0).

Western blot

PNOC expression by Western blot analysis in brainstem and non-brainstem GGs underscored the fact that the protein was expressed in 4 of 5 brainstem GGs, but only one of 4 non-brainstem GGs (Fig. 2).

DISCUSSION

Brainstem GGs are a rare subset of “other” GGs located outside the temporal lobe. Symptoms generated by these tumors are largely related to anatomical location. We conducted a review of the literature and identified a total of 55 cases of GGs involving the brainstem, affecting both pediatric and adult patients. Common presenting symptoms in brainstem tumors included hemiparesis or monoparesis [7], headache, dizziness, and vomiting [5–7]. The age of diagnosis ranged from 3 – 59 years (median 13 years, n=27). The time from onset of symptoms to diagnosis ranged from 2 weeks –15 years (median = 2 years n = 20). There was slight observed male gender preference, with 62% of reported patients being male (n=27) [1,2,5–9,18–27]. This gender preference was not borne out in our data. Tumor diameter on MRI image ranged from 15–75 millimeters (median =40 mm, n=15) [8,9].

Pediatric brainstem GG patients were found to generally have poorer outcomes than pediatric patients with supratentorial GGs [10]. We confirmed this poor outcome in our current series, with recurrence occurring 6 of 7 patients and death in 2 of 7 patients with brainstem GGs, despite chemo- and radiotherapy (see Table I).

Using gene expression microarray technology we further identified a significantly different gene expression signature in brainstem GGs. It was notable that many of these genes with higher expression in brainstem GGs were related to embryogenesis and development.

The largest upregulation in gene expression observed was a 256-fold increase in prepronociceptin transcripts. Prepronociceptin (PNOC) is a precursor protein to nociceptin, the opioid-like agonist of opioid receptor-like (ORL_1) receptor. PNOC has been identified as a functionally-ambiguous component in early mammalian nervous system development

[19], and aberrant PNOC expression has been identified in microarray data of other cancers [20]. The role of prepronociceptin in tumorigenesis, however, is unknown.

A 2006 study by Zaveri *et al.* showed treatment of neuroblastoma cell lines with cAMP analogues in NS20Y neuroblastoma cells induced up to a 200-fold increase in PNOC mRNA. They also reported that a high level of PNOC transcript in undifferentiated neural cells was accompanied by neurite outgrowth [13]. A series of publications by Saito *et al.* additionally demonstrated that transfection of NS20Y cells with PNOC mRNA alone was enough to increase neurite outgrowth, independent of cAMP [14–16]. However, the mature nociceptin peptide did not induce the same change, suggesting that the prehormone itself, or a yet-to-be-discovered modification of the prehormone, is capable of inducing neurite growth [14–16].

PNOC IHC expression was strongest in the neoplastic neurons of brainstem GGs, weaker in 4 of 5 non-brainstem GGs (where it also labeled fewer numbers of neoplastic neurons) and was completely negative in brainstem autopsy samples from normal controls. PNOC IHC expression in GGs was directly compared with IHC expression for NeuN, anti-neurofilament, and synaptophysin and found to be clearly superior to NeuN and neurofilament IHC in identifying neoplastic neurons, especially in brainstem examples. The superiority of PNOC IHC over synaptophysin IHC was less striking but in some cases, it was also easier to interpret PNOC IHC immunoreactivity than synaptophysin IHC immunostaining patterns. This was particularly true in synaptophysin-rich gray matter areas where the cytoplasmic immunoreactivity of PNOC throughout the neuronal cytoplasm was more confidently interpreted as positive. In addition, PNOC appeared to decorate at least as many, if not more, neoplastic neurons than synaptophysin. These results will have to be verified with larger numbers of non-brainstem GG cases. However, our results raise the possibility of utilizing PNOC IHC for diagnostic histopathological purposes in everyday practice.

Gangliogliomas of the brainstem have proven far more difficult to successfully treat when compared to their non-brainstem counterparts. This may be in part due to location but may also be as a result of their unique gene expression. The increased PNOC expression in brainstem GGs offers a unique target for the evaluation of new therapeutic agents. Targeted therapies directed at PNOC exist. Interestingly, drugs such as the anti-neoplastic antibiotic mithramycin A have been shown to be capable of down-regulating PNOC expression *in vitro* [13]. It remains unclear as to whether this drug would have any value in treatment of progressive brainstemGGs. Continued research into the role of PNOC may be of both diagnostic significance and could conceivably provide a new target for chemotherapeutics.

Supplementary Material

Refer to Web version on PubMed Central for supplementary material.

Acknowledgments

The authors thank Mrs. Diane Hutchinson for manuscript preparation and Ms. Lisa Litzenberger for expert photographic work. Financial support for this project was provided by the Morgan Adams Foundation.

References

1. Zhang D, Henning TD, Zou LG, et al. Intracranial ganglioglioma: clinicopathological and MRI findings in 16 patients. Clin Radiol. 2008; 63(1):80–91. [PubMed: 18068794]
2. Westwood DA, MacFarlane MR. Pontomedullary ganglioglioma: a rare tumour in an unusual location. J Clin Neurosci. 2009; 16(1):108–110. [PubMed: 19013803]
3. Louis, DNOH.; Wiestler, OD.; Cavenee, WK., editors. WHO Classification of Tumours of the Central Nervous System. Lyon: International Agency for Research on Cancer; 2007. p. 103
4. DeMarchi R, Abu-Abed S, Munoz D, et al. Malignant ganglioglioma: case report and review of literature. J Neurooncol. 2011; 101(2):311–318. [PubMed: 20524041]
5. Lagares A, Gomez PA, Lobato RD, et al. Ganglioglioma of the brainstem: report of three cases and review of the literature. Surg Neurol. 2001; 56(5):315–322. discussion 322–314. [PubMed: 11750003]
6. Manning HL, Leiter JC. Respiratory control and respiratory sensation in a patient with a ganglioglioma within the dorsocaudal brain stem. Am J Respir Crit Care Med. 2000; 161(6):2100–2106. [PubMed: 10852794]
7. Miller DC, Lang FF, Epstein FJ. Central nervous system gangliogliomas. Part 1: Pathology. J Neurosurg. 1993; 79(6):859–866. [PubMed: 8246054]
8. Park YS, Kim DS, Shim KW, et al. Factors contributing to resectability and seizure outcomes in 44 patients with ganglioglioma. Clin Neurol Neurosurg. 2008; 110(7):667–673. [PubMed: 18499337]
9. Baussard B, Di Rocco F, Garnett MR, et al. Pediatric infratentorial gangliogliomas: a retrospective series. J Neurosurg. 2007; 107(4 Suppl):286–291. [PubMed: 17941492]
10. Lang FF, Epstein FJ, Ransohoff J, et al. Central nervous system gangliogliomas. Part 2: Clinical outcome. J Neurosurg. 1993; 79(6):867–873. [PubMed: 8246055]
11. Ashburner M, Ball CA, Blake JA, et al. Gene ontology: tool for the unification of biology. The Gene Ontology Consortium. Nat Genet. 2000; 25(1):25–29. [PubMed: 10802651]
12. Dennis G Jr, Sherman BT, Hosack DA, et al. DAVID: Database for Annotation, Visualization, and Integrated Discovery. Genome Biol. 2003; 4(5):P3. [PubMed: 12734009]
13. Zaveri NT, Waleh N, Toll L. Regulation of the prepronociceptin gene and its effect on neuronal differentiation. Gene. 2006; 384:27–36. [PubMed: 16935438]
14. Saito Y, Maruyama K, Saido TC, et al. N23K, a gene transiently up-regulated during neural differentiation, encodes a precursor protein for a newly identified neuropeptide nociceptin. Biochem Biophys Res Commun. 1995; 217(2):539–545. [PubMed: 7503733]
15. Saito Y, Maruyama K, Kawano H, et al. Molecular cloning and characterization of a novel form of neuropeptide gene as a developmentally regulated molecule. J Biol Chem. 1996; 271(26):15615–15622. [PubMed: 8663129]
16. Saito Y, Maruyama K, Saido TC, et al. Overexpression of a neuropeptide nociceptin/orphanin FQ precursor gene, N23K/N27K, induces neurite outgrowth in mouse NS20Y cells. J Neurosci Res. 1997; 48(5):397–406. [PubMed: 9185664]
17. Lu J, Nozumi M, Takeuchi K, et al. Expression and function of neuronal growth-associated proteins (nGAPs) in PC12 cells. Neurosci Res. 2011; 70(1):85–90. [PubMed: 21238513]
18. Mickle JP. Ganglioglioma in children. A review of 32 cases at the University of Florida. Pediatr Neurosurg. 1992; 18(5–6):310–314. [PubMed: 1476942]
19. Garcia CA, McGarry PA, Collada M. Ganglioglioma of the brain stem. Case report. J Neurosurg. 1984; 60(2):431–434. [PubMed: 6693970]
20. Epstein N, Epstein F, Allen JC, et al. Intractable facial pain associated with a ganglioglioma of the cervicomedullary junction: report of a case. Neurosurgery. 1982; 10(5):612–616. [PubMed: 7099412]
21. Feigin I, Budzilovich GN. Tumors of neurons and their precursors. J Neuropathol Exp Neurol. 1974; 33(4):483–506. [PubMed: 4214344]
22. Friedman WA, Vries JK, Quisling RG. Ganglioglioma of the medulla oblongata. Surg Neurol. 1979; 12(1):105–108. [PubMed: 451854]

23. Garrido E, Becker LF, Hoffman HJ, et al. Gangliogliomas in children. A clinicopathological study. Childs Brain. 1978; 4(6):339–346. [PubMed: 679771]

24. Gleckman AM, Smith TW. Sudden unexpected death from primary posterior fossa tumors. Am J Forensic Med Pathol. 1998; 19(4):303–308. [PubMed: 9885921]

25. Karamitopoulou E, Perentes E, Probst A, et al. Ganglioglioma of the brain stem: neurological dysfunction of 16-year duration. Clin Neuropathol. 1995; 14(3):162–168. [PubMed: 7671459]

26. Patel U, Pinto RS, Miller DC, et al. MR of spinal cord ganglioglioma. AJNR Am J Neuroradiol. 1998; 19(5):879–887. [PubMed: 9613504]

27. Pollack IF, Hoffman HJ, Humphreys RP, et al. The long-term outcome after surgical treatment of dorsally exophytic brain-stem gliomas. J Neurosurg. 1993; 78(6):859–863. [PubMed: 8487066]

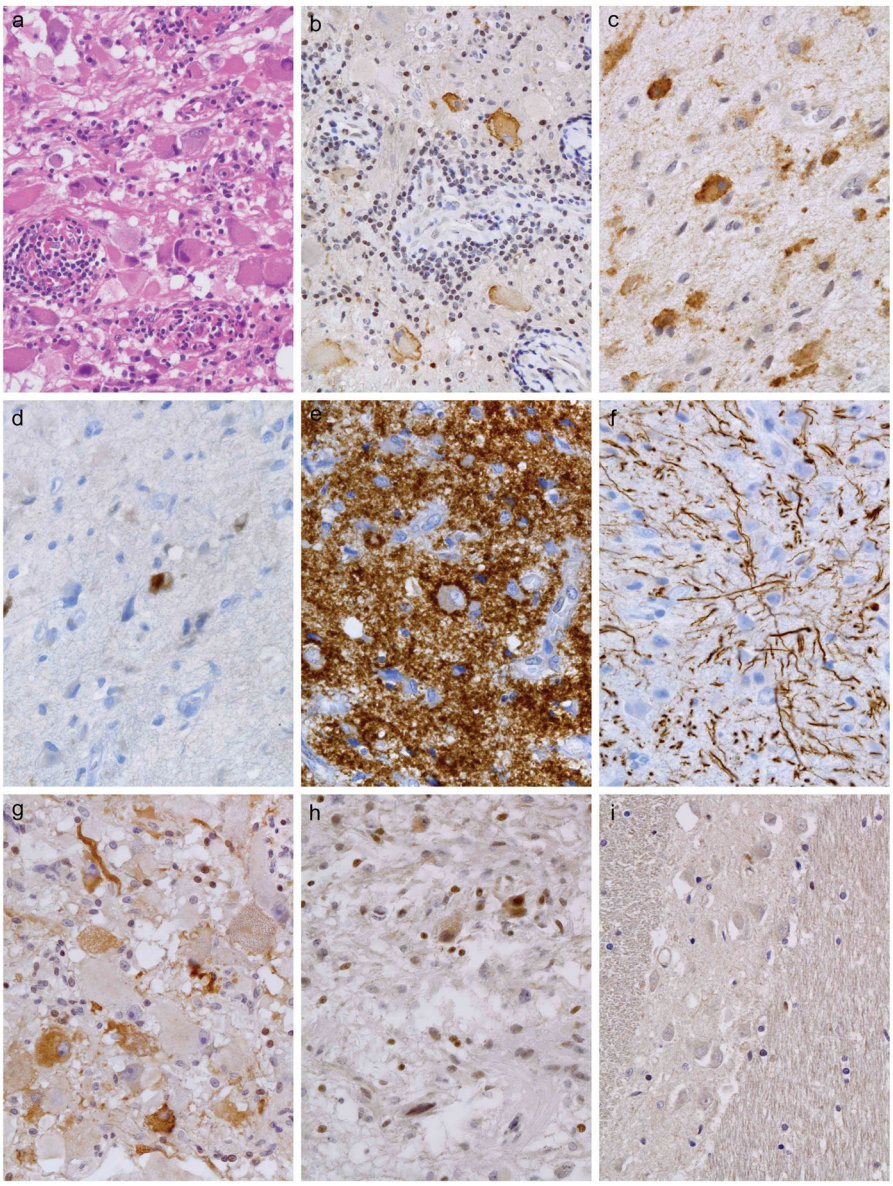

Figure 1.

(a) All brainstem gangliogliomas were classified as WHO grade I and manifested classic histological features of GG on light microscopy, with numerous cytologically-atypical neurons, a low-grade glial component, and variable amounts of perivascular non-neoplastic lymphocytic cuffing (lower left). Hematoxylin and eosin, 400X; Patient 5 from Table I illustrated. **(b)** Immunohistochemical staining for PNOC protein revealed strong (scored as +++) expression in large numbers of neoplastic neurons in all 7 of the brainstem GGs; IHC for PNOC with light hematoxylin counterstain, 400X; Patient 5 from Table I illustrated. **(c)** Immunostaining for PNOC in brainstem gangliogliomas was predominantly cytoplasmic and was distributed throughout the cytoplasm. IHC for PNOC with light hematoxylin counterstain, 600X; Patient 7 from Table I illustrated. **(d)** Careful matching of serial sections taken from the same tissue block from the same case was undertaken to directly compare

similar areas of the tumor in terms of quality of PNOC [see 1c], versus for NeuN, as illustrated in this image. PNOC [see 1c] highlighted the cell body, similar to NeuN [this Fig.] but showed immunostaining in a considerably larger number of the neoplastic neurons. IHC for NeuN with light hematoxylin counterstain, 600X; Patient 7 from Table I illustrated. **(e)** Immunostaining for synaptophysin was strong in the background of the gray-matter rich brainstem; compare this heavy IHC+ background with that for PNOC [see 1c] in the same area of the tumor. Because synaptophysin tended to identify increased synaptic density at the cell membrane/perimeter it was sometimes more difficult to confidently identify IHC+ neoplastic neurons with this immunostain than it was for PNOC. IHC for synaptophysin with light hematoxylin counterstain, 600X; Patient 7 from Table I illustrated. **(f)** Immunostaining for neurofilament predominantly highlighted axons in brainstem gangliogliomas and not cell bodies, as seen in this image. Indeed, unlike neurofilament immunohistochemistry that decorates axons and only occasional cell perikarya in GGs, PNOC did not appear to decorate axonal processes [see 1c for comparison]. IHC for neurofilament with light hematoxylin counterstain, 600X; Patient 7 from Table I illustrated. **(g)** PNOC IHC in non-brainstem gangliogliomas (GGs) was similar to that in brainstem GGs in only 1 of 5 cases, as illustrated in this image, although even in this example, the number of immunoreactive neurons appeared fewer than with brainstem GGs (scored as ++). IHC for PNOC with light hematoxylin counterstain, 400X; Patient 5 from Supplemental Table I illustrated. **(h)** PNOC IHC was significantly weaker and more infrequent in the remaining 2 of 5 non-brainstem GGs, as illustrated in this photomicrograph (scored as +). IHC for PNOC with light hematoxylin counterstain, 400X; Patient 10 from Table II illustrated. **(i)** No observable PNOC expression was found in any brainstem neurons at any level (midbrain, pons, or medulla) of control autopsy specimens; note the negative immunostaining (scored as 0) and clean background in these basis pontis neurons. IHC for PNOC with light hematoxylin counterstain, 400X.

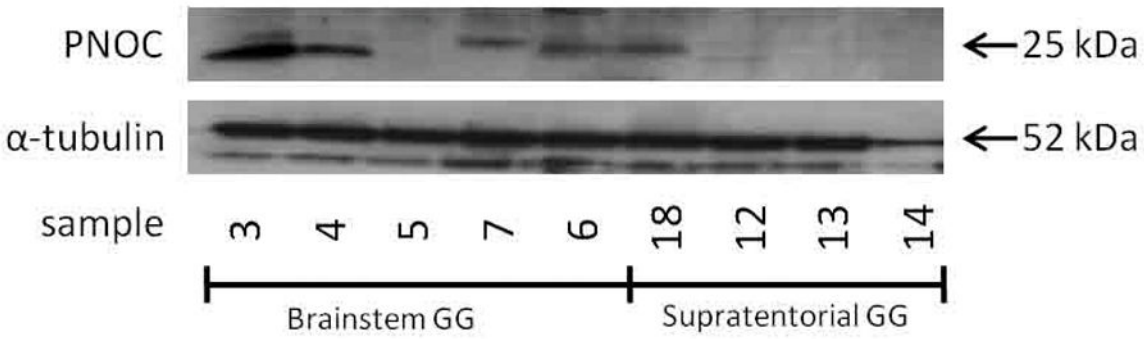

Figure 2.

Western blot analysis of Prepronociceptin (PNOC). Protein lysate (40 ug) from 5 brainstem GGs and 4 supratentorial GGs were probed with anti-PNOC antibody. Anti-A-tubulin antibody was used as an internal control for protein loading.

Table I

Brainstem gangliogliomas: clinical features, , microarray analysis, and PNOC immunoreactivity.

Sample ID	Age and sex	Tumor location	Presenting symptoms	Therapy	Outcome	Recurrent (time to recurrence)	Microarray analysis	PNOC IHC score
1.	4 year-old male	CB/BS/CC	Weakness, respiratory distress, soft voice	C/R	Deceased	Yes (23 months)	no	+++
2.	13 year-old female	CB/BS/CC	Left-sided hearing loss	R	Alive	No	no	+++
3.	3 year-old male	BS/CC	Choking, soft voice, right arm neglect	C/R	Deceased	Yes (9 months)	yes	+++
4.	4 year-old female	CC/BS	Respiratory distress, unsteady gait, soft voice	C/R	Alive	Yes (3 months)	yes	+++
5.	5 year-old male	CB/BS	Uncoordinated left extremity, speech delay	C/R	Alive	Yes (14 months)	yes	+++
6	12-year old female	BS	Weakness, loss of sensation in right hand	C/R	Alive	Yes (19 months)	yes	+++
7.	2 day old female	BS	Facial nerve palsy, left arm weakness	C	Alive	Yes (5 months)	yes	+++

Key: CB=cerebellum, BS=brainstem, CC=cervical spinal cord, C = chemotherapy, R = radiotherapy, WT = wild type; PNOC IHC scoring: +++=strong and diffuse in large numbers of neurons, ++ = strong in a subset of neurons, + = weak and diffuse, +/− = rare neurons with weak immunoreactivity, 0 = none.

Table II

Ten highest upregulated and down-regulated genes in brainstem gangliogliomas versus non-brainstem gangliogliomas, ranked in order of fold change.

Top Upregulated Genes				
Gene Symbol	**Gene Name**	**Probe ID**	**Fold Increase**	**P-value**
PNOC	Prepronociceptin	205901_at	256.9	0.000365
DLX1	Distal-less homeobox1	242138_at	119.8	0.000241
NTS	Neurotensin	206291_at	119.3	0.0442
SIX6	SIX homeobox 6	207250_at	105.0	0.000116
AQP1	Aquaporin 1 (Colton blood group)	207542_s_at	77.4	0.00275
SFRP1	Secreted frizzled-related protein 1	202037_s_at	69.4	0.00548
CRABP1	Cellular retinoic acid binding protein 1	205350_at	67.3	0.0441
PAX3	Paired box 3	231666_at	67.2	0.0000646
RAB3B	RAB3b, member of RAS oncogene family	205924_at	63.4	0.00317
HOXA5	Homeobox A5	213844_at	61.1	0.0291

Top Down-regulated Genes				
Gene Symbol	**Gene Name**	**Probe ID**	**Fold Decrease**	**P-value**
FOXG1	Forkhead box G1	206018_at	69.9	0.0138
MIA	Melanoma inhibitory activity	206560_s_at	45.0	0.00192
NR2E1	Nuclear receptor subfamily 2, group E, member 1	207443_at	36.2	0.0000115
IGF2	Insulin-like growth factor 2 (somatomedin A)	210881_s_at	31.4	0.0146
FOSB	FBJ murine osteosarcoma viral oncogene homolog B	202768_at	28.9	0.0153
ARX	Aristaless related homeobox	238878_at	27.8	0.0468
ADAMTS8	ADAM metallopeptidase with thrombospondin type 1	220677_s_at	25.2	0.000747
C6orf37	Chromosome 6 open reading frame 142	202410_x_at	22.0	0.0160
CABP7	Calcium binding protein 7	235377_at	21.2	0.00785
CHI3L1	Chitinnase 3-like 1 (cartilage glycoprotein-39)	243173_at	19.1	0.0107

Pediatr Blood Cancer. Author manuscript; available in PMC 2015 December 16.

Table III

DAVID ontology analysis of microarray data showing expression of embryonic genes in pediatric brainstem GGs

GOterm	GOterm ID*	P-value
Embryonic skeletal system development	0048706	1.1E-9
Chordate embryonic development	0043009	9.7E-9
Embryonic development ending in birth	0009792	1.8E-8
Embryonic skeletal system morphogenesis	0048704	3.8E-7
Pattern specification process	0007389	3.9E-7
Regionalization	0003002	7.3E-7
Embryonic morphogenesis	0048598	1.1E-6
Anterior/posterior pattern formation	0009952	1.7E-6
Epithelial tube morphogenesis	0060562	1.4E-2

Key

* Gene ontology terms (GOterms) are listed in order of statistical significance.